10956 *Inorg. Chem.* **2010**, *49*, 10956–10959
DOI: 10.1021/ic101351b

Inorganic Chemistry
Article

Analysis of the Magnetic Structure and Ferroelectric Polarization of Monoclinic $MnSb_2S_4$ by Density Functional Theory Calculations

Chuan Tian,[†] Changhoon Lee,[†] Erjun Kan,[†] Fang Wu,[†,‡] and Myung-Hwan Whangbo*[,†]

[†]*Department of Chemistry, North Carolina State University, Raleigh, North Carolina 27695-8204, United States, and* [‡]*School of Science, Nanjing Forestry University, Nanjing, Jiangsu 210037, People's Republic of China*

Received July 7, 2010

Monoclinic $MnSb_2S_4$ consists of MnS_4 chains made up of edge-sharing MnS_6 octahedra and adopts a (0, 0.369, 0) magnetic superstructure below 25 K. This ordered magnetic structure, in which the spins of each MnS_4 chain possess a helical spin arrangement, has C_2' symmetry. On the basis of density functional theory calculations, we explored the origin of the observed noncollinear spin arrangement of $MnSb_2S_4$ by evaluating its spin exchanges to find that spin exchanges are frustrated not only within each MnS_4 chain but also between adjacent MnS_4 chains. Our analysis predicts that $MnSb_2S_4$ is a multiferroic with a ferroelectric polarization of $\sim$14 $\mu C/m^2$ along the chain direction, and a field-induced reversal of the ferroelectric polarization of $MnSb_2S_4$ can occur by reversing the direction of the helical spin rotation in each MnS_4 chain.

1. Introduction

For a crystalline solid to have ferroelectric (FE) polarization, it should not possess inversion symmetry.[1,2] A magnetic solid that exhibits FE polarization is commonly referred to as a multiferroic. In principle, a noncentrosymmetric magnetic solid can have FE polarization independent of its magnetic structure. A centrosymmetric magnetic solid can lose inversion symmetry either by cooperative second-order Jahn–Teller distortion or by chiral magnetic order.[1−3] For a one-dimensional (1D) magnetic chain, Katsura et al. showed that a cycloidal spiral-spin order (in which the propagation vector of the chain lies in the plane of the spin rotation) leads to FE polarization, but neither a helical spiral-spin order (in which the propagation vector of the chain is perpendicular to the plane of the spin rotation) nor a sinusoidal spiral-spin order does.[4] However, if chains with helical spiral-spin order interact strongly to form a three-dimensional (3D) magnetic structure whose overall symmetry is C_2 (2-fold rotational symmetry) or C_2' (i.e., C_2 plus time reversal), then FE polarization occurs along the rotational axis.[5] A further symmetry analysis[6] showed that FE polarization also occurs even when the magnetic structure has no symmetry other than identity if it is composed of building blocks with symmetry m (mirror-plane symmetry) or m' (i.e., m plus time reversible), with the FE polarization lying in the mirror plane. So far, the phenomenon of magnetic-order-induced FE polarization has been found predominantly among transition-metal magnetic oxides. To our knowledge, the layered disulfide $AgCrS_2$[7] is the only reported example of a multiferroic not based on transition-metal oxides. It is of interest to find more examples of nonoxide-based multiferroics induced by chiral magnetic order.

Manganese diantimony sulfide $MnSb_2S_4$ occurs in two different polymorphs, i.e., orthorhombic[8] and monoclinic[9] phases. Both polymorphs consist of MnS_4 chains that are made up of edge-sharing MnS_6 octahedra. In each MnS_4 chain of the monoclinic phase, every shared S atom plus its two adjacent unshared S atoms make a SbS_3 trigonal pyramid, leading to a $MnSb_2S_4$ chain (Figure 1a), and such $MnSb_2S_4$ chains are packed together to form the 3D lattice of monoclinic $MnSb_2S_4$ (Figure 1b). In the orthorhombic phase, the SbS_3 trigonal pyramids are made within each MnS_4 chain as well as between MnS_4 chains to make strongly

*To whom correspondence should be addressed. E-mail: mike_whangbo@ncsu.edu.

(1) (a) Ramesh, R.; Spaldin, N. A. *Nat. Mater.* **2007**, *6*, 21. (b) Khomskii, D. *Physics* **2009**, *2*, 20.
(2) (a) Eerenstein, W.; Mathur, N. D.; Scott, J. F. *Nature* (*London*) **2006**, *442*, 759. (b) Cheong, S. W.; Mostovoy, M. *Nat. Mater.* **2007**, *6*, 13. (c) Tokura, Y. *J. Magn. Magn. Mater.* **2007**, *310*, 1145.
(3) Kan, E. J.; Xiang, H. J.; Lee, C.; Wu, F.; Yang, J. L.; Whangbo, M.-H. *Angew. Chem., Int. Ed.* **2010**, *49*, 1603.
(4) Katsura, H.; Nagaosa, N.; Balatsky, A. *Phys. Rev. Lett.* **2005**, *95*, 057205.
(5) Arima, T.-H. *J. Phys. Soc. Jpn.* **2007**, *76*, 073702.
(6) Kan, E. J.; Xiang, H. J.; Zhang, Y.; Lee, C.; Whangbo, M.-H. *Phys. Rev. B* **2009**, *80*, 104417.
(7) Singh, K.; Maignan, A.; Martin, C.; Simon, Ch. *Chem. Mater.* **2009**, *21*, 5007.
(8) Bente, K.; Edenharter, A. *Z. Kristallogr.* **1989**, *186*, 31.
(9) Pfitzer, A.; Kurowski, D. *Z. Kristallogr.* **2000**, *215*, 373.

 Published on Web 11/01/2010

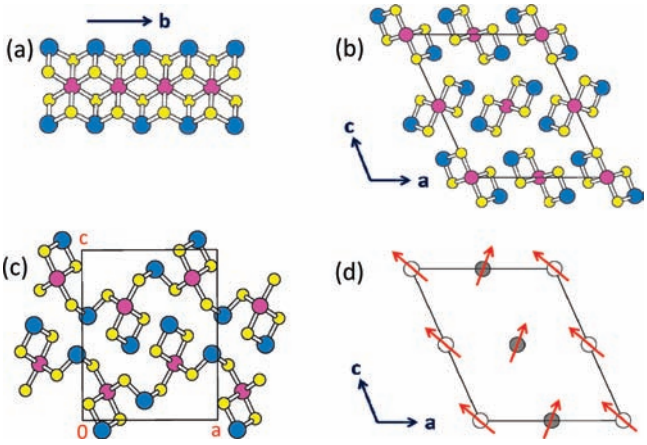

Figure 1. Crystal and magnetic structures of $MnSb_2S_4$: (a) $MnSb_2S_4$ chain of monoclinic $MnSb_2S_4$, which results from a MnS_4 chain of edge-sharing MnS_6 octahedra capped with SbS_3 pyramids. The pink, purple, and yellow spheres (the large, medium, and small circles, respectively) represent Mn, Sb and S, respectively. (b) Projection view of $MnSb_2S_4$ chains in monoclinic $MnSb_2S_4$ along the *b* direction. (c) Projection view of $MnSb_2S_4$ layers in orthorhombic $MnSb_2S_4$ along the *b* direction, where SbS_3 pyramids cap each MnS_4 chain and interconnect between adjacent MnS_4 chains. (d) Spin arrangement of the $MnSb_2S_4$ chains in monoclinic $MnSb_2S_4$. The chains are represented by showing only the Mn atoms. The unshaded and shaded circles, representing the Mn atoms, differ in their *b*-axis height by *b*/2.

corrugated $MnSb_2S_4$ layers, which are packed to form the 3D lattice of orthorhombic $MnSb_2S_4$ (Figure 1c). Matar et al.[10] examined the electronic structures of both $MnSb_2S_4$ phases on the basis of density functional theory (DFT) calculations within the local spin density approximation. Their study showed that both phases are antiferromagnetic (AFM) semiconductors, in agreement with the available experimental results.[9,11] However, the magnetic structure of monoclinic $MnSb_2S_4$ below its 3D AFM ordering temperature T_N = 25 K is not collinear but exhibits a helical arrangement along each MnS_4 chain (see below).[11]

The magnetic properties of monoclinic $MnSb_2S_4$ arise from the high-spin Mn^{2+} ($S = {}^5/_2$) ions. With the Curie–Weiss temperature $\theta = -63$ K and the Néel temperature $T_N = 25$ K,[9] the spin frustration in $MnSb_2S_4$ is moderate because the ratio $f = |\theta|/T_N$ is considerably smaller than 6.[12] Nevertheless, the ordered magnetic structure of monoclinic $MnSb_2S_4$ below T_N, determined by powder neutron diffraction,[11] shows a noncollinear spin arrangement that is typically observed from magnetic systems with strong spin frustration; the spins of each MnS_4 chain have a helical rotation along the chain (i.e., along the *b* direction) with propagation vector $\mathbf{q} = (0, 0.369, 0)$, while the spins between adjacent chains have a ferromagnetic (FM) arrangement along the *c* direction but have a ~70°-rotated arrangement along the *a* direction (Figure 1d).[11] The noncollinear spin arrangements along the *b* and *a* directions indicate the existence of spin frustration not only along each MnS_4 chain but also between adjacent MnS_4 chains. Furthermore, the overall symmetry of this magnetic structure is C_2' with each

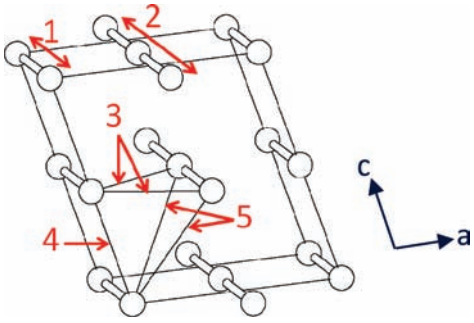

Figure 2. Five spin-exchange paths J_1–J_5 of monoclinic $MnSb_2S_4$. For simplicity, only the Mn atoms are shown as circles. The circles joined by cylinders represent the MnS_4 chains along the *b* direction. The numbers 1–5 refer to the spin-exchange paths J_1–J_5, respectively.

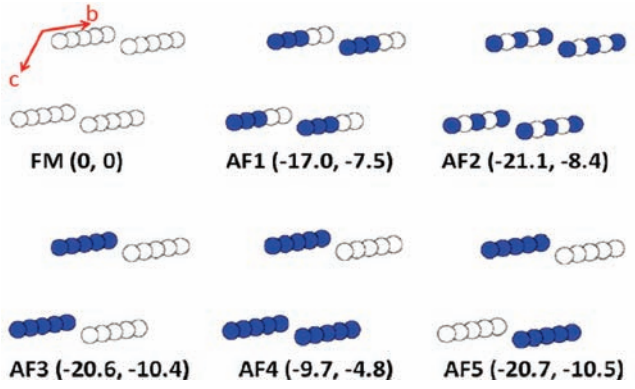

Figure 3. Six ordered spin states of monoclinic $MnSb_2S_4$ defined in terms of the (*a*, 5*b*, *c*) supercell, where the unshaded and shaded circles represent the up-spin and down-spin Mn^{2+} sites, respectively. The numbers in each parenthesis (from left to right) refer to the relative energies (in meV per 4 FUs) determined from GGA+U calculations with U_{eff} = 4 and 6 eV, respectively.

MnS_4 chain as the rotational axis. This suggests that monoclinic $MnSb_2S_4$ is a nonoxide-based multiferroic with its FE polarization along the chain direction. In the present work, we verify this suggestion and analyze the noncollinear magnetic order of monoclinic $MnSb_2S_4$ causing FE polarization on the basis of DFT electronic structure calculations.

2. Computational Details

To analyze the magnetic structure of monoclinic $MnSb_2S_4$, it is necessary to determine its spin exchanges. We evaluate the five exchanges J_1–J_5 of $MnSb_2S_4$ defined in Figure 2 by performing DFT calculations for the six ordered spin states constructed with a (*a*, 5*b*, *c*) supercell (Figure 3). In our calculations, the experimental crystal structure[9] of monoclinic $MnSb_2S_4$ was employed with no further structure optimization. Our DFT calculations employed the frozen-core projector augmented wave method encoded in the Vienna ab initio simulation packages[13] and the generalized-gradient approximation (GGA)[14] with a plane-wave-cutoff energy of 400 eV and a set of six *k* points for the irreducible Brillouin zone. To properly describe the effect of electron correlation in the Mn 3d states, the GGA plus on-site repulsion method

(10) Matar, S. F.; Weihrich, R.; Kurowski, D.; Pfitzner, A.; Eyert, V. *Phys. Rev. B* **2005**, *71*, 235207.
(11) Leone, P.; Doussier, C.; Andre, G.; Moelo, Y. *Phys. Chem. Miner.* **2008**, *35*, 201.
(12) (a) Greedan, J. E. *J. Mater. Chem.* **2001**, *11*, 37. (b) Dai, D.; Whangbo, M.-H. *J. Chem. Phys.* **2004**, *121*, 672.
(13) (a) Kresse, G.; Hafner, J. *Phys. Rev. B* **1993**, *47*, 558. (b) Kresse, G.; Furthmüller, J. *Comput. Mater. Sci.* **1996**, *6*, 15. (c) Kresse, G.; Furthmüller, J. *Phys. Rev. B* **1996**, *54*, 11169.
(14) Perdew, J. P.; Burke, K.; Ernzerhof, M. *Phys. Rev. Lett.* **1996**, *77*, 3865.

Table 1. Mn···Mn Distances (in Å) Associated with the Spin-Exchange Paths J_1−J_5 of Monoclinic $MnSb_2S_4$ and the Values of J_1/k_B−J_5/k_B (in K) Determined from GGA+U Calculations with U_{eff} = 4 and 6 eV

	Mn···Mn (Å)	U_{eff} = 4 eV	U_{eff} = 6 eV
J_1/k_B	3.799	−2.18	−0.44
J_2/k_B	7.598	−2.80	−1.43
J_3/k_B	6.651	−2.54	−1.31
J_4/k_B	7.553	0.28	0.19
J_5/k_B	7.890	0.15	0.10

(GGA+U)[15] was used with the effective $U_{eff} = U - J$ values of 4 and 6 eV, typical values used for Mn.[16]

To simulate the electronic structure of the ordered magnetic state of $MnSb_2S_4$ below T_N, we approximate its $\mathbf{q}$ = (0, 0.369, 0) incommensurate structure with the $\mathbf{q}$ = (0, $^1/_3$, 0) commensurate one and carry out GGA+U calculations with spin−orbit coupling (SOC) interactions included. The resulting electronic structure is used to calculate the FE polarization of $MnSb_2S_4$ by employing the Berry phase method.[17] The observed magnetic structure is chiral; i.e., the helical spin rotation in each MnS_4 chain is right-handed along the positive b direction. Thus, we approximate the observed magnetic structure by the $\mathbf{q}$ = (0, $^1/_3$, 0) commensurate structure with the helical rotation angle ϕ = +120°. We also consider the $\mathbf{q}$ = (0, $^1/_3$, 0) commensurate structures with ϕ = 0° and −120° to see if the FE polarization of $MnSb_2S_4$ can be reversed in sign by changing the direction of the helical rotation angle ϕ.

3. Spin Exchanges and Magnetic Structure

Among the five spin exchanges defined in Figure 2, J_1 and J_2 are the spin exchanges along each MnS_4 chain and J_3−J_5 are the interchain interactions between adjacent MnS_4 chains. The Mn···Mn distances associated with these exchange paths are summarized in Table 1. The relative energies of the six ordered spin states determined by GGA+U calculations are summarized in Figure 3. In terms of the spin Hamiltonian

$$\hat{H} = -\sum_{i<j} J_{ij}\hat{S}_i \cdot \hat{S}_j \qquad (1)$$

where $J_{ij} = J_1$−J_5, the total spin-exchange energies per formula unit (FU) of these states are obtained as

$$\begin{aligned}
&\text{FM}: && (-4J_1 - 4J_2 - 8J_3 - 4J_4 - 8J_5)(N^2/4)\\
&\text{AF1}: && (-4J_1 + 12J_2 - 26J_3 - 4J_4 - 26J_5)(N^2/20)\\
&\text{AF2}: && (+12J_1 - 4J_2 - 6J_3 - 4J_4 - 6J_5)(N^2/20)\\
&\text{AF3}: && (-4J_1 - 4J_2 + 8J_3 - J_4 + 8J_5)(N^2/4)\\
&\text{AF4}: && (-4J_1 - 4J_2)(N^2/4)\\
&\text{AF5}: && (-4J_1 - 4J_2 + 8J_3 + 4J_4 - 8J_5)(N^2/4)
\end{aligned} \qquad (2)$$

by applying the energy expressions obtained for spin dimers with N unpaired spins per spin site (in the present case, N = 5).[18] Thus, when the relative energies of the six ordered spin states determined by the GGA+U calculations are mapped onto the corresponding relative energies determined from the above spin-exchange energies, we obtain the values of J_1−J_5 summarized in Table 1. The spin exchanges calculated with the larger U_{eff} are smaller in magnitude than those with the smaller U_{eff}, as is generally found for other magnetic solids.[6,16,19] In terms of these exchanges, one can calculate the Curie−Weiss temperature θ of $MnSb_2S_4$ in the mean-field approximation[20]

$$\theta \approx \frac{20(J_1 + J_2 + J_3 + J_4 + J_5)}{k_B} \qquad (3)$$

to obtain θ = −142 and −57.8 K by using the spin exchanges determined from GGA+U calculations with U_{eff} = 4 and 6 eV, respectively. These values are in reasonable agreement with the experimental value of −63 K. Thus, our GGA+U calculations with U_{eff} = 4 overestimated the spin exchanges by a factor of approximately 2. In general, GGA+U calculations are known to overestimate the spin exchanges of magnetic oxides.[18a,21]

Table 1 shows that the nearest-neighbor and next-nearest-neighbor intrachain exchanges (J_1 and J_2, respectively) are both AFM, so the spin exchanges along each MnS_4 chain are frustrated, as found for the CuO_2 ribbon chains of $LiCuVO_4$ and $LiCuO_2$[22] and for the $CuCl_2$ ribbon chains of $CuCl_2$.[23] The spins of these CuO_2 and $CuCl_2$ ribbon chains (of edge-sharing CuO_4 and $CuCl_4$ square planes, respectively) have a cycloidal spiral-spin arrangement in their ordered magnetic states, while those of the MnS_4 chains have a helical spiral-spin arrangement in their ordered magnetic states. The spiral-spin order of cycloidal or helical type occurs to reduce the spin frustration generated by J_1 and J_2, which occurs when $J_1 > 0$ and $J_2 < 0$ or when $J_1 < 0$ and $J_2 < 0$. In terms of the classical spin approximation for an isolated 1D chain defined by J_1 and J_2, the propagation vector $\mathbf{q}$ of the spiral-spin structure is related to the J_1/J_2 ratio as[24]

$$\mathbf{q} = \frac{1}{2\pi}\arccos\left(-\frac{J_1}{4J_2}\right) \qquad (4)$$

from which we find $\mathbf{q}$ = 0.281 and 0.262 by using the J_1/J_2 values obtained from the GGA+U calculations with U_{eff} = 4 and 6 eV, respectively. These values are somewhat smaller than the experimental value of 0.369. The discrepancy should not be surprising because the interchain spin exchanges J_3−J_5 are not taken into consideration in this analysis.

Of the three interchain spin exchanges J_3−J_5, J_3 is nearly as strongly AFM as the intrachain exchange J_2, whereas J_4 and J_5 are weakly FM (Table 1). As depicted in Figure 1c, the adjacent chains along the c direction have a FM arrangement but have a ∼70°-rotated arrangement along the a direction.

(15) Dudarev, S. L.; Botton, G. A.; Savrasov, S. Y.; Humphreys, C. J.; Sutton, A. P. *Phys. Rev. B* **1998**, *57*, 1505.
(16) Tian, C.; Lee, C.; Xiang, H. J.; Zhang, Y.; Payen, C.; Jobic, S.; Whangbo, M.-H. *Phys. Rev. B* **2009**, *80*, 104426.
(17) (a) King-Smith, R. D.; Vanderbilt, D. *Phys. Rev. B* **1993**, *47*, 1651. (b) Resta, R. *Rev. Mod. Phys.* **1994**, *66*, 899.
(18) (a) Dai, D.; Whangbo, M.-H. *J. Chem. Phys.* **2001**, *114*, 2887. (b) Dai, D.; Whangbo, M.-H. *J. Chem. Phys.* **2003**, *118*, 29.
(19) (a) Xiang, H. J.; Lee, C.; Whangbo, M.-H. *Phys. Rev. B: Rapid Commun.* **2007**, *76*, 220411(R). (b) Koo, H.-J.; Whangbo, M.-H. *Inorg. Chem.* **2008**, *47*, 128. (c) Koo, H.-J.; Whangbo, M.-H. *Inorg. Chem.* **2008**, *47*, 4779.
(20) Smart, J. S. *Effective Field Theory of Magnetism*; Saunders: Philadelphia, PA, 1966.
(21) (a) Dai., D.; Koo, H.-J.; Whangbo, M.-H. *J. Solid State Chem.* **2003**, *175*, 341. (b) Dai, D.; Whangbo, M.-H.; Koo, H.-J.; Rocquefelte, X.; Jobic, S.; Villesuzanne, A. *Inorg. Chem.* **2005**, *44*, 2407. (c) Grau-Crespo, R.; de Leeuw, N. H.; Catlow, C. R. *J. Mater. Chem.* **2003**, *13*, 2848.
(22) Xiang, H. J.; Whangbo, M.-H. *Phys. Rev. Lett.* **2007**, *99*, 257203.
(23) Banks, M. G.; Kremer, R. K.; Hoch, C.; Simon, A.; Ouladdiaf, B.; Broto, J.-M.; Rakoto, H.; Lee, C.; Whangbo, M.-H. *Phys. Rev. B* **2009**, *80*, 024404.
(24) Dai, D.; Koo, H.-J.; Whangbo, M.-H. *Inorg. Chem.* **2004**, *43*, 4026.

The noncollinear spin arrangement along the *a* direction indicates that the interchain spin exchanges along the *a* direction are frustrated. Indeed, the spin exchanges in the (J_1, J_3, J_3), (J_1, J_5, J_5), and (J_3, J_4, J_5) triangles, which occur between adjacent MnS_4 chains, are frustrated (Figure 2). The spins have an FM arrangement along the *c* direction in the observed magnetic structure, which can be related to the minimization of the spin frustration in the (J_3, J_4, J_5) triangles. Every J_4 magnetic bond makes two different (J_3, J_4, J_5) triangles, and J_5 is weaker than J_4 by a factor of approximately 2 (Table 1), so that the FM spin arrangement along the *c* direction minimizes the interchain interaction energy, $2J_3 + J_4 + 2J_5$, per two (J_3, J_4, J_5) triangles.

4. FE Polarization

In general, the polarization P of an FE compound below a certain temperature T_N is a relative value, namely, the polarization below T_N minus that above T_N. In addition, the polarization of an FE compound should reverse its sign when the applied electric field E is reversed in direction below T_N. This is explained in terms of a double-well potential energy curve as a function of E for the transformation from one FE structure with $P > 0$ through a paraelectric (PE) structure with $P = 0$ to an alternative FE structure with $P < 0$. In the absence of the helical magnetic order along each MnS_4 chain (i.e., $\phi = 0°$), the magnetic structure of monoclinic $MnSb_2S_4$ is centrosymmetric. Therefore, when the sign of the electric field E is switched, the polarization of monoclinic $MnSb_2S_4$ might reverse its sign by reversing the sense of the helical spin rotation along each MnS_4 chain, as has been considered for the multiferroic $Ba_3NbFe_3Si_2O_{14}$ with helical spiral-spin order.[25]

To confirm the above points, we perform GGA+U+SOC calculations for the (0, $^1/_3$, 0) superstructures of $MnSb_2S_4$ with the helical spin rotation angles $\phi = +120°$, 0°, and $-120°$. The relative energies of the three structures are 13, 26, and 0 meV per Mn for $\phi = -120°$, 0°, and $+120°$, respectively. Namely, the right-handed helical spin rotation ($\phi = +120°$) is energetically more stable than the left-handed helical spin rotation ($\phi = -120°$). This is consistent with the experimental observation[11] and reflects the effect of the interchain spin-exchange interactions. The (0, $^1/_3$, 0) superstructure with $\phi = 0°$ is less stable than those with $\phi = -120°$ and $+120°$ because of the intrachain spin frustration. Our subsequent Berry phase calculations for the (0, $^1/_3$, 0) superstructures show that $P = -14.2$, 0, and 12.3 $\mu C/m^2$ for $\phi = +120°$, 0°, and $-120°$, respectively. (Here the positive and negative polarizations are directed along the positive and negative *b* directions, respectively). Thus, the (0, $^1/_3$, 0) superstructure with $\phi = 0°$ represents the PE structure of $MnSb_2S_4$, and the FE polarization of $MnSb_2S_4$ is approximately $-14\ \mu C/m^2$ and can change its sign by reversing the direction of the helical spin rotation.

5. Concluding Remarks

Our GGA+U calculations reveal that the spin exchanges of monoclinic $MnSb_2S_4$ are frustrated not only within each MnS_4 chain but also between adjacent MnS_4 chains. This explains the occurrence of the helical spin arrangement in each MnS_4 chain and the noncollinear spin arrangement between adjacent MnS_4 chains along the *a* direction. $MnSb_2S_4$ is predicted to be a multiferroic with FE polarization $P \approx -14\ \mu C/m^2$ along the MnS_4 chain direction. A field-induced reversal of the FE polarization of $MnSb_2S_4$ is expected to occur by reversing the direction of the helical spin rotation in each MnS_4 chain. It should be noted that the spin exchanges between adjacent MnS_4 chains are substantial in $MnSb_2S_4$, which explains why $MnSb_2S_4$ can be a multiferroic in spite of a helical spiral-spin order in each MnS_4 chain.

Acknowledgment. This work was supported by the Office of Basic Energy Sciences, Division of Materials Sciences, U.S. Department of Energy, under Grant DE-FG02-86ER45259, and also by the computing resources of the NERSC center and the HPC center of NCSU. M.-H.W. thanks Christophe Payen and Stéphane Jobic for invaluable discussion during the development of this work.

(25) Lee, C.; Kan, E. J.; Xiang, H. J.; Whangbo, M.-H. *Chem. Mater.* **2010**, *22*, 5290.